

Received January 1, 2021, accepted January 17, 2021, date of publication January 28, 2021, date of current version February 8, 2021.

Digital Object Identifier 10.1109/ACCESS.2021.3055236

Single-Phase Fault Line Selection in Distribution Network Based on Signal Injection Method

LIN NIU¹, GUIQING WU, AND ZHANGSHENG XU

College of Electrical and Information Engineering, Hunan University, Changsha 410082, China

Corresponding author: Lin Niu (niulin@hnu.edu.cn)

This work was supported by the State Grid Hunan Electric Power Research Institute of China under Grant 1619SE-WZ.

ABSTRACT The distribution network with small current grounding mode can ensure high power supply reliability, but it is difficult to locate single-phase grounding fault line. Most of the faults in distribution network are single-phase to ground fault. It is important to locate the fault line timely and accurately for the normal operation of the power grid. In this article, a fault line selection method based on signal injection is proposed. The dynamic selection of parameters and injection frequency in real-time monitoring distribution network by injection method is analyzed. The accuracy of signal frequency domain conversion is improved by using all phase Fourier transform. Taking the active power consumption of injected signal after fault as the criterion, the accuracy of line selection is improved. Through theoretical analysis and simulation, as well as experiments in a 600V distribution system, the fault line can be accurately selected.

INDEX TERMS Fault line selection, signal injection method, non-effectively earthed neutral, single-phase to ground fault.

I. INTRODUCTION

In the early stage of the development of distribution network, the system capacity is small. The power equipment adopts the operation mode of neutral point direct grounding. However, with the continuous development of industrialization, the scale of distribution network is also expanding. When single-phase ground fault occurs, the grounding current of neutral point is very large. The circuit breaker will trip as a whole, resulting in power failure [1]. In order to solve this problem, China's power industry adopts the operation mode of ungrounded or grounded by arc suppression coil at the neutral point of distribution network. Also known as small current grounding mode [2]. When single-phase to ground fault occurs, the line voltage is still balanced. The mode has the characteristics of short-term operation with fault and provides a certain time for fault line selection.

Single-phase to ground fault accounts for more than 70% of all grid faults, and most of the phase to phase faults are caused by the untimely single-phase fault treatment [3]. After the single-phase fault occurs in the small current grounding system, the line voltage is still consistent with that before the fault. However, if the fault line is not selected in time, the increased fault phase voltage may damage the insula-

tion. It leads to the expansion of fault scope and affects the safety and stability of the whole distribution network system. In recent years, with the development of urban distribution network, underground cables are widely used. The capacitance current generated by the distributed capacitance to the ground is multiplied. Therefore, the operation mode of neutral point grounding through arc suppression coil is generally adopted in large capacity distribution network. It can also be called resonant grounding system [4]. The capacitive current of distribution network is compensated by arc suppression coil, which can effectively reduce the fault current in single-phase grounding fault and avoid the generation of arc. However, due to the complex characteristics of resonant grounding system, the realization of fault line selection is more difficult.

The existing fault line selection equipment and algorithm can be divided into two aspects, passive line selection and active line selection [5]. Among them, the passive line selection is based on the steady-state signal and transient signal of the power grid fault. A line selection method based on current reactive component is proposed in [6], [7], while negative-sequence and zero-sequence voltages are used in [8]. However, most distribution networks have their neutral points grounded through arc suppression coil. Because of the function of arc suppression coil, it is difficult to realize the original fault zero-sequence criterion. Reference [9] uses

The associate editor coordinating the review of this manuscript and approving it for publication was Zhiyi Li¹.

wavelet transform to select fault line from transient signals of non-fault line and fault line after fault, and [10]–[12] propose using wavelet transform to select line with energy analysis. Reference [13] uses negative selection algorithm (NSA) and Hilbert Huang transform (HHT) to analyze the transient information. Because of the short duration of fault transient process, it is difficult to sample data. The accuracy of the passive route selection method is difficult to guarantee, and the engineering implementation is also difficult.

Signal injection method is a type of active line selection [14]. When single-phase to ground fault occurs, signal injection method is used to inject signal from external signal source. The fault line selection can be realized by sampling and analyzing the injection signals of each line. Reference [15] measures the capacitive current of distribution network by injecting signal from the open triangle side of voltage transformer. But this method will introduce the error of leakage resistance and reactance. In [16]–[18], a signal injection method without external signal source is proposed. After the fault occurs, the resistance is connected to the neutral point of the distribution network, which increases the zero-sequence active power of the fault line. However, this method can only connect the resistance to the neutral point after the fault, which has great interference to the distribution network system. References [19], [20] propose to inject DC signal to detect the size of DC component of each line to realize line selection. However, DC signal is vulnerable to interference after injection. The injected AC sinusoidal signal is used in [21], [22]. The amplitude of the injected signal remains unchanged, but the frequency changes in a certain range. After getting the resonance frequency of the system, the parameters of the distribution network are calculated. However, the frequency range of this method is limited, and the resonance frequency of distribution network may not be in its range. In [23], [24], signal injection method is used for fault line selection, but the influence of injection frequency is not considered. In [25], it is proposed that power frequency 50 Hz signal is injected to locate the fault by the change of zero-sequence voltage and current. However, the 50 Hz signal injected into the distribution network will increase the fault current and threaten the insulation safety of the system. The frequency of sinusoidal AC signal injected in [26]–[29] is 220 Hz. It is pointed out that the third harmonic (150 Hz) has a large interference. The frequency selection method avoids harmonic interference, but it is difficult to realize line selection when the grounding resistance is large.

In order to solve the above problems, a fault line selection method based on AC signal injection is proposed. During the normal operation of the distribution network, the parameters of the distribution network are monitored in real time through periodic signal injection and analysis. The mathematical model is extracted to detect the operation changes of the distribution network. After the fault occurs, the injection signal frequency is dynamically selected according to the previous distribution network system model. In this way, more injection signals flow into the fault line and improve the

accuracy of line selection. In sampling signal processing, all phase Fast Fourier Transform (APFFT) is adopted to solve the problem of spectrum leakage caused by non-integer sampling period. The spectrum of injection signal can be obtained completely [30]–[34]. The active power consumption of the injected signal in each line is used as the fault line selection criterion to improve the anti-interference ability.

The rest of this article is organized as follows: Section II analyses the principle of signal injection method. In Section III, the real-time monitoring algorithm of each parameter in the normal operation of distribution network is proposed. Section IV describes the algorithm of dynamic selection of signal frequency after fault. In section V, APFFT is proposed to process the sampled signal and obtain the spectrum. In section VI, criterion of fault line selection is proposed. Section VII and Section VIII are the analysis of simulation and experiment results respectively. Conclusions are drawn in Section IVV.

II. FAULT LINE SELECTION PRINCIPLE OF SIGNAL INJECTION METHOD

The schematic diagram of fault line selection by signal injection method is shown in Fig. 1, which shows the distribution network system with N outgoing lines. When the switch K is disconnected, the distribution network operates in the mode of neutral point ungrounded. When K is closed, the distribution network operates in resonant grounding mode. G point is the ground fault point, R_G is the grounding transition resistance. The neutral point of distribution network is led out from the grounding transformer. An external signal source

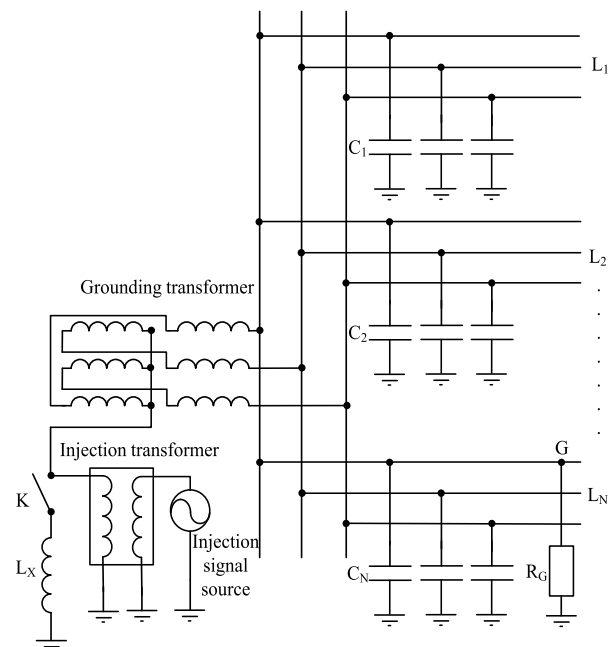


FIGURE 1. Schematic diagram of fault line selection by signal injection method.

with controllable frequency is connected and injected into the transformer to access the neutral point.

The three-phase parameters of grounding transformer and each line are usually symmetrical. The three-phase distributed capacitance to ground can be considered to be basically equal. Therefore, the amplitude and phase of the three-phase current induced by the injection current at the high-voltage side of the grounding transformer are equal. The injected current and its voltage can be analyzed according to the zero-sequence signal. After the current signal is injected from the injection transformer, the current signal with the same frequency will be generated through the grounding transformer at the high-voltage side of the distribution network. It will generate zero-sequence voltage with corresponding frequency in the grounding transformer and the line.

When the distribution network works normally, the neutral point voltage is close to zero. When the current signal is injected into the neutral point, the distribution network parameters can be calculated by sampling the voltage and current values at the injected signal. In this article, the mathematical models of ungrounded neutral point system and resonant grounding system are established respectively to realize the real-time parameter monitoring of distribution network. In case of single-phase fault, the neutral point voltage will rise to the maximum phase voltage under normal condition.

After the grounding fault occurs, the neutral point voltage changes suddenly. The signal source injects a certain frequency signal into the distribution network, and samples the voltage vector and current vector at the injection end. Then the signal is sampled at the starting point of each outgoing line. Since the frequency of the injected signal is selected according to the real-time data of the distribution network, more injected signals will flow into the fault point. By analyzing the injection signal of each line, fault line selection can be realized.

The signal injection method adopts the secondary side to monitor the comprehensive parameters of the distribution network and fault line selection, which has high security. The interference of primary side operation on the normal operation of power grid is avoided, and the security risk is reduced.

III. REAL TIME MONITORING OF DISTRIBUTION NETWORK PARAMETERS

In order to realize the dynamic selection of injection signal frequency for fault line selection, the mathematical model of distribution network in normal operation should be extracted in real time. The existing monitoring methods of distribution network parameters need to be measured at the primary side when the distribution network stops working. This method will affect the continuity of power supply. There is a certain deviation between the measurement of parameters when the distribution network stops running and the actual operation. In this article, three frequency injection signal method is proposed to monitor the parameters of distribution network in

real time under the normal operation. The method can ensure the power supply continuity of the distribution network. The measurement process of on-line monitoring distribution network parameters by signal injection method does not involve the primary side of the system. Even in normal operation, there is no hidden danger of high voltage, which can ensure the safety of personnel and equipment.

Fig. 2 shows the equivalent circuit model of resonant grounding system. Sampling is conducted at the same time of signal source injection. \dot{I} is the injected current and \dot{U} is the voltage generated by the injected current.

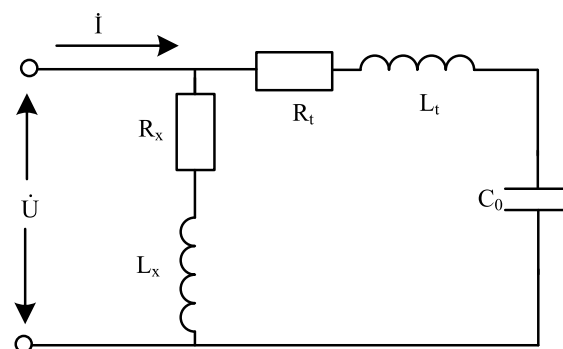


FIGURE 2. Overall equivalent circuit diagram of distribution network system.

As shown in Fig. 2, R_x is the equivalent resistance of the arc suppression coil, L_x is the equivalent inductance of the arc suppression coil, R_t is the equivalent resistance of the grounding transformer and the line, L_t is the equivalent inductance of the grounding transformer, and C_0 is the overall distributed capacitance to the ground of the distribution network.

A. PARAMETERS MONITORING OF UNGROUNDED NEUTRAL SYSTEM

The traditional distribution network with small capacity still adopts the neutral point ungrounded operation, without considering the effect of arc suppression coil. The equivalent circuit of the system is shown in Fig. 3, and the parameters are defined as shown in Fig. 2.

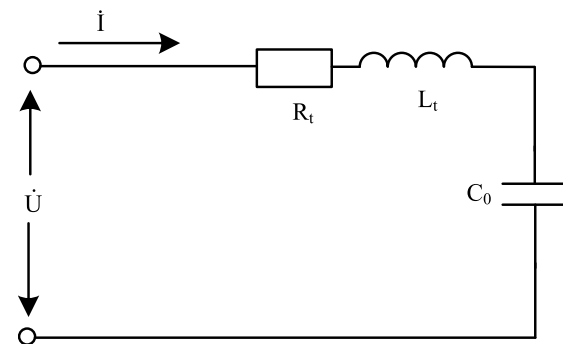


FIGURE 3. Equivalent circuit diagram of neutral ungrounded system.

The impedance value Z of the whole system is as follows:

$$Z = \frac{\dot{U}}{\dot{I}} = R_t + j\omega L_t + \frac{1}{j\omega C_0} \quad (1)$$

where, $\omega = 2\pi f$, f is the frequency of the injected signal. Three current signals with constant amplitude and frequency of ω_1 , ω_2 and ω_3 are injected into the neutral point of distribution network in three times. Three corresponding zero-sequence voltages can be measured at the injected signals. Then the impedance Z_1 , Z_2 , and Z_3 of the system can be calculated when the signal is injected three times, as shown in equation (2).

$$\begin{cases} |Z_1|^2 = R_t^2 + (\omega_1 L_t - \frac{1}{\omega_1 C_0})^2 \\ |Z_2|^2 = R_t^2 + (\omega_2 L_t - \frac{1}{\omega_2 C_0})^2 \\ |Z_3|^2 = R_t^2 + (\omega_3 L_t - \frac{1}{\omega_3 C_0})^2 \end{cases} \quad (2)$$

The total distributed capacitance C_0 of the system can be calculated by the impedance formula corresponding to the three injections in equation (2), as shown in equation (3).

$$C_0 = \left[\frac{\omega_1^2(|Z_2|^2 - |Z_3|^2) + \omega_2^2(|Z_3|^2 - |Z_1|^2) + \omega_3^2(|Z_1|^2 - |Z_2|^2)}{(\omega_3^2 - \omega_2^2)/\omega_1^2 + (\omega_1^2 - \omega_3^2)/\omega_2^2 + (\omega_2^2 - \omega_1^2)/\omega_3^2} \right]^{-\frac{1}{2}} \quad (3)$$

B. PARAMETER MONITORING OF NEUTRAL RESONANT GROUNDING SYSTEM

At present, most of the distribution network lines put into use are grounded by arc suppression coil, which makes online monitoring more difficult. At present, the on-line monitoring of the operation mode parameters needs to be carried out by using the measurement method of neutral point ungrounded system after the arc suppression coil is out of operation. In this article, the admittance model of the system is established after the triple frequency signal is injected. The real-time data monitoring of distributed capacitance and arc suppression coil is realized in the distribution network with the neutral resonant grounding in normal operation. Convert the circuit shown in Fig. 2 into admittance model, as shown in Fig. 4.

Where, R_x' is the admittance value of arc suppression coil impedance, L_x' is the admittance value of arc suppression coil inductance, R_t' is the admittance value of grounding transformer and line impedance, L_t' is the admittance value of inductive reactance of grounding transformer and line, and C_0' is the admittance value of distributed capacitance reactance. According to Fig. 2 and Fig. 4, the admittance

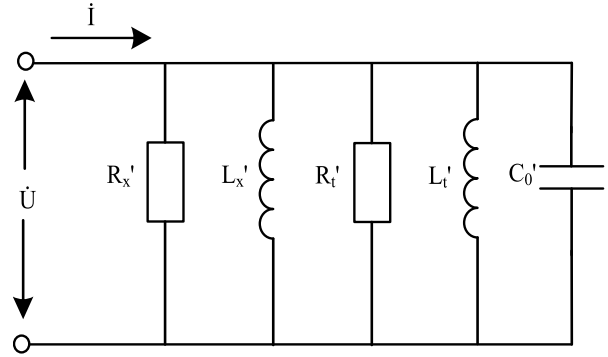


FIGURE 4. Equivalent admittance diagram of neutral resonant grounding system.

values of the above items can be deduced as follows:

$$\begin{cases} R_t' = \frac{R_t}{R_t^2 + (\omega L_t - 1/\omega C_0)^2} \\ C_0' = \frac{j}{\omega C_0 R_t^2 + \omega C_0 (\omega L_t - 1/\omega C_0)^2} \\ L_t' = -\frac{j\omega L_t}{R_t^2 + (\omega L_t - 1/\omega C_0)^2} \\ R_x' = \frac{R_x}{R_x^2 + \omega^2 L_x^2} \\ L_x' = -\frac{j\omega L_x}{R_x^2 + \omega^2 L_x^2} \end{cases} \quad (4)$$

The function of arc suppression coil is to use its inductive reactance to counteract the capacitance reactance of distributed capacitance. Therefore, the reactance value in the impedance model of arc suppression coil is much greater than the resistance value. The reactance value of grounding transformer and distribution network line is also much greater than the resistance value under the action of high frequency signal. Therefore, when calculating the parameters of the injected signals of the distribution network with the neutral resonant grounding, the frequency should be larger (more than 200Hz). When the injection frequency is larger, the relationship between R_x , R_t , L_x and L_t is shown in equation (5).

$$\begin{cases} \omega^2 L_x^2 \gg R_x^2 \\ (\omega L_t - \frac{1}{\omega C_0})^2 \gg R_t^2 \end{cases} \quad (5)$$

Replace the relationship of equation (5) into equation (4). After injecting high frequency signal, the total admittance of the simplified system can be obtained. The admittance value Y is shown in equation (6).

$$Y = \frac{\dot{I}}{\dot{U}} = \frac{R_t}{(\omega L_t - 1/\omega C_0)^2} + \frac{R_x}{\omega^2 L_x^2} + j\left(\frac{\omega C_0}{1 - \omega^2 L_t C_0} - \frac{1}{\omega L_x}\right) \quad (6)$$

The imaginary part of the corresponding system admittance is obtained by injecting three high frequency signals. The imaginary parts B_1 , B_2 and B_3 of the three admittances

are as follows:

$$\begin{cases} B_1 = \frac{\omega_1 C_0}{1 - \omega_1^2 L_x C_0} - \frac{1}{\omega_1 L_x} \\ B_2 = \frac{\omega_2 C_0}{1 - \omega_2^2 L_x C_0} - \frac{1}{\omega_2 L_x} \\ B_3 = \frac{\omega_3 C_0}{1 - \omega_3^2 L_x C_0} - \frac{1}{\omega_3 L_x} \end{cases} \quad (7)$$

The values of arc suppression coil and distributed capacitance can be obtained by connecting the three imaginary parts of admittance in equation (7). The coefficients are as follows:

$$\begin{cases} k_1 = \frac{\omega_3^2(\omega_2^2 - \omega_1^2)}{\omega_2 B_2 - \omega_1 B_1} \\ k_2 = \frac{\omega_2^2(\omega_3^2 - \omega_1^2)}{\omega_3 B_3 - \omega_1 B_1} \\ k_3 = \frac{\omega_1^2(\omega_3^2 - \omega_2^2)}{\omega_3 B_3 - \omega_2 B_2} \end{cases} \quad (8)$$

The inductance L_x of the arc suppression coil is obtained as follows:

$$L_x = \frac{k_2 - k_1}{\omega_1^2(\omega_2^2 - \omega_3^2) + \omega_1 B_1(k_1 - k_2)} \quad (9)$$

The overall distributed capacitance C_0 of distribution network is obtained as follows:

$$C_0 = \frac{(\omega_1^2 - \omega_2^2)(\omega_3^2 - \omega_2^2)(\omega_1^2 - \omega_3^2)}{\omega_1^2(k_2 - k_3)(\omega_2^2 - \omega_3^2) - \omega_3^2(k_1 - k_2)(\omega_1^2 - \omega_2^2)} \quad (10)$$

Since the frequency selection of the injection signal takes into account the signal flow direction on the high voltage side, the main parameters required are the distributed capacitance and arc suppression coil. These parameters can be obtained by (3), (9) and (10).

IV. FREQUENCY OF INJECTED SIGNAL IN FAULT LINE SELECTION

Due to the distributed capacitance in each line of distribution network, the shunt of injected signal is inevitable. In normal operation of distribution network, the proportion of injected signal flowing into each line is directly proportional to the size of distributed capacitance. After single-phase grounding fault in distribution network, the proportion of injected signal flowing into each normal line is also related to the size of distributed capacitance and arc suppression coil. In order to ensure that the signal flows into the fault line as much as possible, different injection frequency should be selected for different distribution network systems.

The two most common forms of small current grounding system are ungrounded neutral point and resonant grounding. Because the mathematical models of the two grounding modes are different, the selection of injection frequency should be analyzed separately from the two grounding modes. Because the three-phase parameters of grounding transformer are symmetrical, the voltage drop formed by injected signal is the same. The distribution network equivalent injection signal flow diagram mainly considers the parallel effect of

distributed capacitance and arc suppression coil. It has been known that the value of distributed capacitance and arc suppression coil can be monitored in real time when the distribution network is working normally.

A. SELECTION OF INJECTION FREQUENCY FOR UNGROUNDED NEUTRAL SYSTEM

After the fault occurs in the ungrounded neutral system, the flow direction of the injected signal in the distribution network system is shown in Fig. 5. Among them, \dot{I}_{in} represents the corresponding value of injection current at primary side, \dot{I}_C represents injection current flowing into distributed capacitance of non-fault line, \dot{I}_G represents injection current flowing into fault point, R_G represents fault grounding resistance of distribution network, and C_0 represents distributed capacitance.

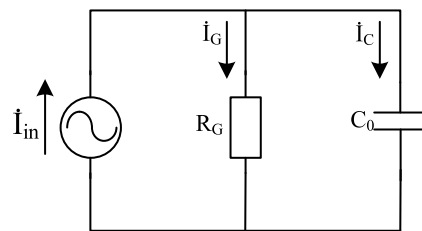


FIGURE 5. Signal flow diagram of ungrounded neutral system.

Therefore, $\dot{I}_{in} = \dot{I}_G + \dot{I}_C$, The current \dot{I}_G flowing into the fault line is:

$$\dot{I}_G = \frac{1}{1 + j\omega C_0 R_g} \dot{I}_{in} \quad (11)$$

The amplitude $|\dot{I}_G|$ of the current flowing into the fault line is shown in (12).

$$|\dot{I}_G| = \frac{1}{\sqrt{1 + (\omega C_0 R_g)^2}} |\dot{I}_{in}| \quad (12)$$

where, $\omega = 2\pi f$, f is the frequency of the injected signal.

From equation (12), it can be seen that in the distribution network system with ungrounded neutral point, low frequency signal should be injected as much as possible to improve the accuracy of fault line selection.

B. SELECTION OF INJECTION FREQUENCY FOR NEUTRAL RESONANT GROUNDING SYSTEM

Resonant grounding is more commonly seen in highly capacitive distribution network. The flow direction of injected signal through arc suppression coil grounding distribution network is shown in Fig. 6.

L_x represents the arc suppression coil and \dot{I}_L represents the injection current flowing into the arc suppression coil. The meaning of other values is the same as that in Fig. 5. Therefore, $\dot{I}_{in} = \dot{I}_G + \dot{I}_C + \dot{I}_L$, the current \dot{I}_G flowing into the fault line is shown in (13).

$$\dot{I}_G = \frac{j\omega L_x}{R_g + j\omega L_x - \omega^2 C_0 L_x R_g} \dot{I}_{in} \quad (13)$$

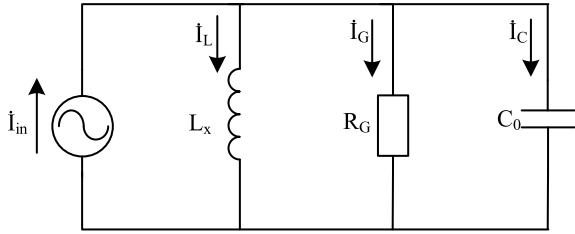


FIGURE 6. Signal flow diagram of neutral resonant grounding system.

The amplitude $|\dot{I}_G|$ of current flowing into the fault line is shown in (14).

$$|\dot{I}_G| = \frac{1}{\sqrt{1 + (\omega C_0 R_g - R_g / \omega L_x)^2}} |\dot{I}_{in}| \quad (14)$$

From the (14), the injection frequency of the maximum amplitude of the injected signal flowing into the fault line can be obtained. The injection frequency f is as follows:

$$f = \frac{1}{2\pi \sqrt{C_0 L_x}} \quad (15)$$

From the above formula (15), it can be seen that the frequency selection of the injected signal of the resonant grounding system makes the arc suppression coil and the distributed capacitance have parallel resonance. Although resonance over-current will appear in inductor and capacitor, they cancel each other, which is equivalent to mutual compensation of reactive power. It will not affect active power judgment for fault line selection. The amplitude of the injected signal is small and the injection time is short, which will not have a great impact on the power grid. The configuration of arc suppression coil in different distribution networks is different, so the corresponding injection frequency should be calculated according to formula (15) combined with the parameters of distribution network.

V. APFFT PROCESSING DATA

In the process of fault line selection based on signal injection method, neutral point voltage in distribution network and the voltage and current value of each outgoing line need to be sampled. Accurate frequency domain transformation of sampled data is an indispensable condition for high-precision fault line selection.

In the process of distribution network data sampling, it means that the signal is truncated, the truncated signal is periodically extended. The Discrete Fourier transform (DFT) and Fast Fourier transform (FFT) can be used to obtain the corresponding frequency domain signal. In the truncation process, because the truncated signal is not the entire period of the original signal, the spectrum leakage phenomenon will occur. The calculated spectrum will have error with the real value. Distribution network fault waveform is very complex, it is difficult to achieve the whole period sampling. It will lead to two adjacent continuation wave form is not smooth

transition, that is to say, truncation error will be introduced. Therefore, APFFT is used to solve the problem of spectrum leakage and get accurate frequency domain data and its own phase invariance. The phase can be obtained without correction.

The core of all phase processing is to reduce the influence of signal truncation error, therefore the truncation at the center of the signal is calculated. N-point APFFT needs $2N - 1$ data for all phase processing which are then divided into N-segment data. The number of each segment is N, and it is added circularly at the center of the data. The all phase preprocessed data of N-point is obtained. Fig. 7 shows the system structure of APFFT.

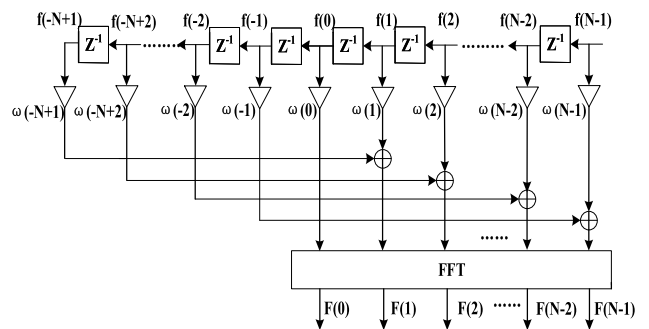


FIGURE 7. APFFT system structure diagram.

The power frequency 50Hz fundamental wave and harmonic signals of power grid mostly exist in the form of sinusoidal signal. Therefore, different sinusoidal signals can be used as the original signal to simulate the actual situation of injecting different frequency signals into the power grid. According to Euler formula, sine signal can be written as exponential signal. Therefore, in order to facilitate the derivation process, it is assumed that the exponential signal is the original signal. The original signal $f(n)$ can be expressed as follows:

$$f(n) = e^{j(\omega_0 n + \varphi_0)} \quad (16)$$

where, $-N \leq n \leq N - 1$. First, the signal is analyzed by ordinary FFT spectrum, and then calculated according to the definition of FFT, as shown in (17). The result $F(K)$ of FFT can be expressed as follows:

$$\begin{aligned} F(k) &= \frac{1}{N} \sum_{n=0}^{N-1} f(n) e^{-j\frac{2\pi}{N}nk} \\ &= \frac{1}{N} \sum_{n=0}^{N-1} e^{j(\frac{2\pi}{N}k_0 n + \varphi_0)} e^{-j\frac{2\pi}{N}nk} \\ &= \frac{1}{N} \frac{\sin[\pi(k_0 - k)]}{\sin[\pi(k_0 - k)/N]} e^{j\varphi_0} e^{j\pi(\frac{N-1}{N})(k_0 - k)} \end{aligned} \quad (17)$$

Next, the spectrum of APFFT is analyzed. APFFT consists of all phase data preprocessing and FFT. All phase processing data is shown in Fig. 7. The all phase preprocessing method

used in this article is that there are still N data after the shift of center cycle $f(0)$, as shown in (18).

$$\begin{aligned}
 f_0 &= [f(0), f(1), \dots, f(N - 1)] \\
 f_1 &= [f(-1), f(0), \dots, f(N - 2)] \\
 &\dots\dots\dots \\
 f_{N-1} &= [f(-N + 1), f(-N + 2), \dots, f(0)] \quad (18)
 \end{aligned}$$

The data after all phase preprocessing is shown in equation (18). According to the linear and frequency shift characteristics of DFT, the data after all phase processing can be equivalent to N groups of original data. After frequency shift, DFT analysis and linear superposition are conducted. Assuming that the discrete Fourier transform corresponding to f_i is $F_i(k)$, the corresponding APFFT result $F_{AP}(K)$ is shown in (19).

$$\begin{aligned}
 F_{AP}(k) &= \frac{1}{N} \sum_{m=0}^{N-1} F_m(k) e^{j\frac{2\pi}{N}mk} \\
 &= \frac{1}{N^2} \frac{\sin^2[\pi(k_0 - k)]}{\sin^2[\pi(k_0 - k)/N]} e^{j\varphi_0} \quad (19)
 \end{aligned}$$

It can be seen from (17) and (19) that the amplitude of APFFT is the square of the amplitude of ordinary FFT, indicating a stronger suppression effect on the side lobe and highlight of the main spectral line in the amplitude spectrum. Therefore, it has a certain effect on suppressing spectrum leakage. Through the formula of APFFT, it can be seen that in the phase spectrum of APFFT, each spectral line corresponds to the initial phase. The phase spectrum of ordinary FFT has spectrum offset. Therefore, the phase spectrum of APFFT can accurately reflect the initial phase without correction.

In MATLAB simulation, five signals are generated and superimposed. The results of APFFT and windowed FFT are shown in Fig. 8 and Fig. 9. The side lobe value of APFFT main spectral line in Fig. 8 is only half of that of FFT. The phase spectrum value of APFFT in Fig. 9 is the initial phase of corresponding frequency signal. However, the original phase spectrum of windowed FFT is not corrected, there is spectrum offset phenomenon. Therefore, the suppression function of APFFT on spectrum leakage and horizontal initial phase characteristics can be verified. APFFT can extract the injection current and voltage vector values more effectively when processing the sampled signal.

VI. FAULT LINE SELECTION CRITERIA

When single-phase grounding fault occurs in distribution network, the injected signal will produce active power and reactive power in each line. But the fault line will consume more active power because of the transition resistance. Therefore, the anti-interference ability of the injection method can be improved by comparing the active power consumption of the injected signal in each line.

When the distribution network works normally, the three phases are balanced and the neutral point voltage is close to zero. After the fault occurs, the three-phase balance is broken

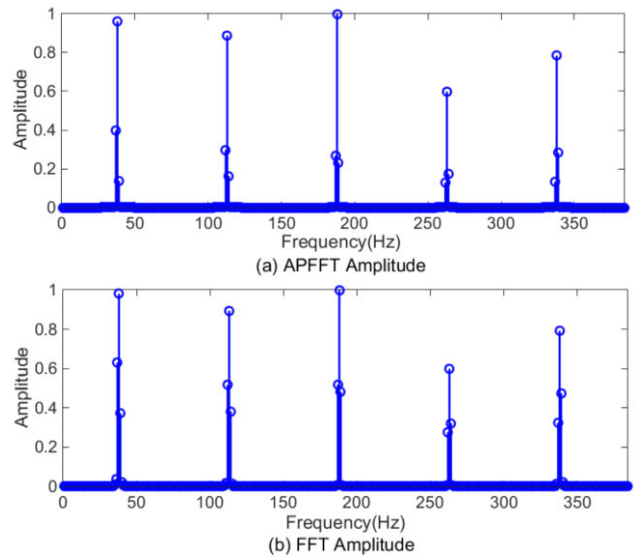


FIGURE 8. Comparison of amplitude spectra between APFFT and FFT.

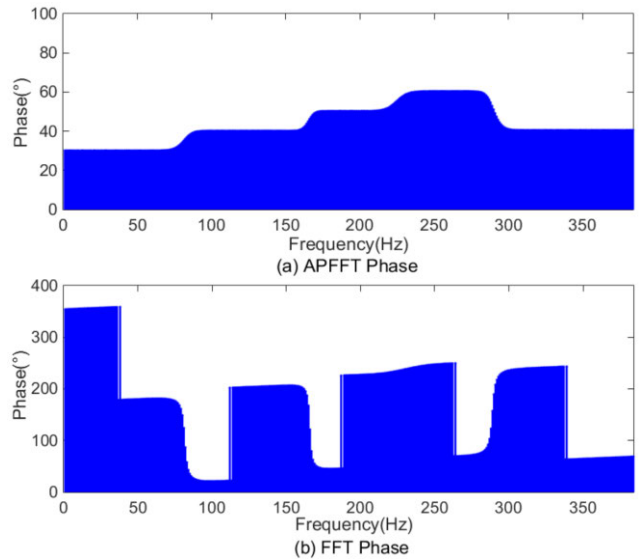


FIGURE 9. Comparison of phase spectra between APFFT and FFT.

and the neutral point voltage is close to the normal phase voltage.

According to the state grid distribution network fault judgment data, the judgment condition of neutral point voltage location fault occurrence is determined. When the neutral point voltage amplitude exceeds 20% of the normal phase voltage amplitude, it is considered that the fault occurs, as shown in equation (20). Where, U_0 is the effective value of neutral point voltage and U_A is the effective value of normal operating phase voltage.

$$U_0 > 20\% * U_A \quad (20)$$

When the power grid is normal, inject the signal with equal interval, and sample the neutral point voltage value U_0 . When

the neutral point voltage is higher than 20% of the normal phase voltage, the signal is injected into the neutral point again immediately. The voltage \dot{U}_i generated by the injection signal in each line is sampled. The injected signal from each line is \dot{I}_i . The angle θ_i between \dot{U}_i and \dot{I}_i is obtained after processing the data by APFFT. The active power consumed P_i by the injected signal in each line is shown in equation (21). Where, $i = 1, \dots, N$, N is the N lines of the distribution network.

$$P_i = |\dot{U}_i| |\dot{I}_i| \cos \theta_i, \quad i = 1, \dots, N \quad (21)$$

The maximum value of P_i is P_a , and the second largest value is P_b . K_f is the judgment value of line selection accuracy, as shown in equation (22). When equation (22) is satisfied, the fault line can be accurately selected. The line corresponding to P_a is the fault line.

$$K_f = \frac{P_a}{P_b} > 1.5 \quad (22)$$

VII. SIMULATION VERIFICATION

A. ESTABLISHMENT OF DISTRIBUTION NETWORK SIMULATION MODEL

The fault line selection simulation is carried out in Matlab/Simulink. The passive method and injection method are respectively simulated. The YJV23 cable is selected after the cable parameters are inquired. The resistance matrix, inductance matrix and capacitance matrix of the simulation are shown in Tab. 1.

TABLE 1. Simulation cable parameters.

Parameter category	$R/(\Omega/km)$	$L/(mH/km)$	$C/(\mu F/km)$
Positive sequence	0.193	0.422	0.143
Zero sequence	1.93	1.477	0.143

In order to simulate the real situation of distribution network, four outgoing lines with different lengths are simulated. The simulation results are analyzed under different neutral operation modes and different grounding resistance.

B. EXTRACTION OF INJECTION SIGNAL BY APFFT

In the actual distribution network fault situation, data sampling will be disturbed by noise. In order to verify the anti-jamming ability of APFFT, noise is added to the injected signal in the simulation process. APFFT is used to extract the injection signal and analyze the error. The signal to noise ratio (SNR) is taken as 10dB. The results are shown in Tab. 2. APFFT has high accuracy for the extraction of injected signals with interference.

C. SIMULATION OF FAULT ZERO-SEQUENCE CURRENT

The steady-state passive method is mainly used in the early development of distribution network, with simple structure and small capacity. Compared with other non-fault lines, the amplitude of zero-sequence current of fault line is the largest, and its phase difference is 180 degrees. The zero-sequence

TABLE 2. Simulation of APFFT effect.

Parameter category	Theoretical value	Measured value	Error
Frequency/(Hz)	60	59.454	0.91%
Amplitude/(A)	1	0.986	1.34%
Phase/(°)	30	29.98	0.07%

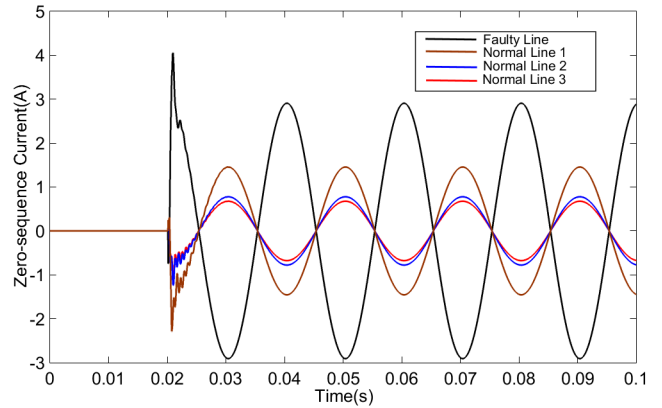


FIGURE 10. Fault zero-sequence current diagram of ungrounded neutral system.

current waveform of each line after fault is shown in Fig. 10. It can be seen that the amplitude and phase of zero-sequence current of fault line are different from those of the three normal lines. The zero-sequence current of normal line is also different due to the difference of line length and parameters.

At present, resonant grounding operation mode is generally adopted in large capacity distribution network. Arc suppression coil is connected to neutral point to compensate distributed capacitance, so as to reduce capacitance current caused by grounding fault. However, due to the compensation of arc suppression coil, the amplitude and phase of zero-sequence current of each line are irregular in steady state. Therefore, it is difficult to realize accurate line selection by steady-state method. The zero-sequence current after resonance grounding system fault is shown in Fig. 11.

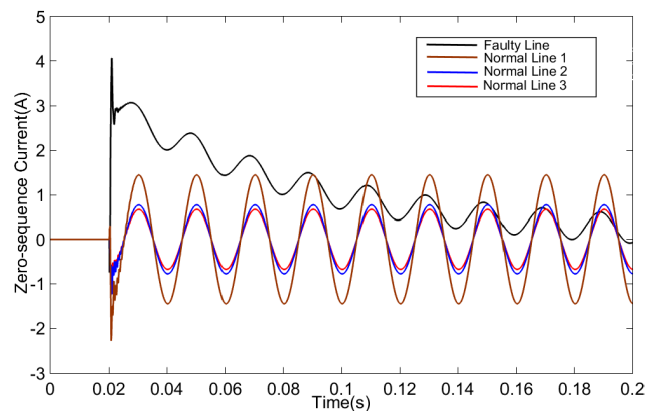


FIGURE 11. Fault zero-sequence current diagram of neutral resonant grounding system.

At the moment of fault, the zero-sequence current of fault line is the largest. The compensation of arc suppression coil makes the grounding current decrease rapidly. Therefore, the fault line cannot be identified according to the amplitude phase relationship. In theory, the transient passive method is effective, to solve the problem of single-phase fault in resonant grounding distribution system. However, the transient process is generally short after the fault occurs, which makes it difficult to sample the fault waveform in engineering. As shown in Fig. 10 and Fig. 11, the transient process after the fault occurs is only tens of microseconds. The signal injection time and sampling time of the active line selection method can be controlled, and the influence of fault on the accuracy of line selection is minimal.

D. SIMULATION OF DISTRIBUTION NETWORK PARAMETER MONITORING

In order to verify the accuracy of three frequency injection method in distribution network parameter monitoring, different distribution network parameters are set for simulation in neutral ungrounded and resonant grounded systems. At the beginning of the simulation, the distribution network is in normal operation. At this time, the signal is injected three times and the values of distributed capacitance and arc suppression coil are calculated according to equation (3), (9) and (10). The results are shown in Tab. 3 and Tab. 4. Where, C_0 and L_0 are simulation set values of distributed capacitance and arc suppression coil respectively, C_1 and L_1 are simulation measured values of distributed capacitance and arc suppression coil respectively. E_C is the measurement error of distributed capacitance and E_L is the measurement error of arc suppression coil, as shown in equation (23).

$$\begin{cases} E_C = \frac{C_1 - C_0}{C_0} * 100\% \\ E_L = \frac{L_1 - L_0}{L_0} * 100\% \end{cases} \quad (23)$$

From Tab. 3 and Tab. 4, it can be seen that the injected three frequency signal method has high accuracy in parameter monitoring of normal distribution network.

TABLE 3. Parameter monitoring of ungrounded neutral system.

$C_0/\mu F$	$C_1/\mu F$	E_C
3.165	3.190	0.79%
5.883	5.931	0.82%
16.538	16.676	0.84%
33.853	34.055	0.60%
60.496	60.713	0.36%

TABLE 4. Parameter monitoring of neutral resonant grounding system.

$C_0/\mu F$	L_0/mH	$C_1/\mu F$	L_1/mH	E_C	E_L
3.165	2613.357	3.119	2627.469	-1.45%	0.54%
5.883	878.709	5.802	882.927	-1.38%	0.48%
16.538	425.103	16.319	426.845	-1.32%	0.41%
33.853	369.015	33.456	370.122	-1.17%	0.30%
60.496	116.308	59.721	116.691	-1.28%	0.33%

E. EFFECT OF INJECTION FREQUENCY SELECTION

The distribution network system corresponding to 16.538 μF distributed capacitance in Tab. 3 and Tab. 4 is selected for simulation. The frequency of the injected signal is dynamically selected by equation (12) and equation (15) respectively for the neutral ungrounded system and resonant grounded system. The frequency of the injected signal is 10Hz for the neutral ungrounded system and 60Hz for the resonant grounded system. In order to compare the advantages of dynamic selection of injection signal frequency, the 220 Hz injection frequency used in [26]–[29] and the injection frequency in this article are simulated. Combined with the fault line selection criteria in section VI, the two frequency selection effects are compared.

P_G is the active power consumption of fault line injection signal, and P_N is the active power consumption of all injection signals. In order to compare the effect of frequency selection, the parameter K_{in} represents the proportion of active power consumption of fault line injection signal in the whole. K_{in} is defined as follows:

$$K_{in} = \frac{P_G}{P_N} * 100\% \quad (24)$$

The active power consumption ratio of the injected signal at different frequencies is shown in Fig. 12 and Fig. 13. When the fault ground resistance is large, it is difficult to realize high resistance line selection with 220 Hz fixed frequency injection signal. The method of dynamic selection of injection signal frequency can greatly improve the accuracy of fault line selection.

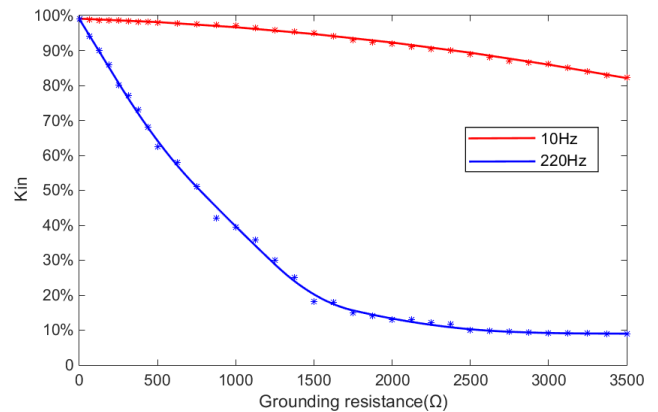


FIGURE 12. Effect of injection frequency selection in ungrounded neutral system.

F. SIMULATION OF FAULT LINE SELECTION

In order to verify the effect of fault line selection algorithm in this article, the traditional fault line selection method is compared with the proposed method. In [26]–[29], 220 Hz injection signal is used, and the corresponding line selection criterion is the maximum value of each line injected signal. The criterion of fault line selection in this article is the active power consumption of injected signal in each line. In order

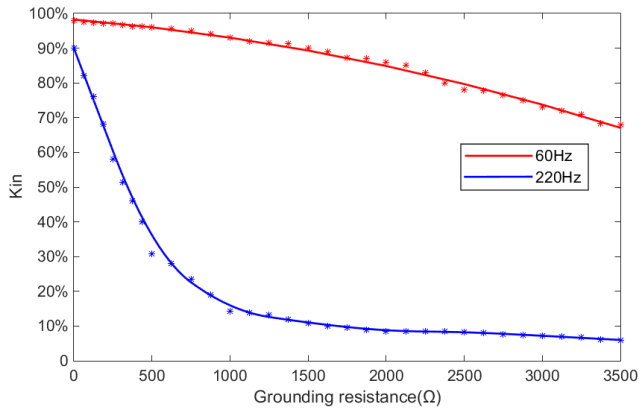


FIGURE 13. Effect of injection frequency selection in neutral resonant grounding system.

to compare the difference between the method in [26]–[29] and the method in this article, equation (25) is the judging mark of accurate line selection in [26]–[29]. Where, I_a is the maximum value of each line injected signal, and I_b is the second largest value of each line injected signal. The size of K_S represents the accuracy of traditional injection method. K_S is defined as follows:

$$K_S = \frac{I_a}{I_b} > 1.5 \quad (25)$$

On the basis of the above simulation, the amplitudes of injected signals corresponding to the four lines after 220 Hz injection signal rate are I_1, I_2, I_3 and I_4 respectively. The corresponding line selection criterion K_S is calculated according to equation (25). When equation (25) is satisfied, the result of fault line selection is correct. The corresponding results of the two distribution network systems are shown in Tab. 5 and Tab. 6.

The simulation sets the first line as the fault line and the rest lines as the normal line. When the fault grounding

TABLE 5. Fault line selection based on fixed frequency and amplitude comparison in ungrounded neutral system.

R_G/Ω	I_1/A	I_2/A	I_3/A	I_4/A	K_S
50	1.08	0.01	0.02	0.01	54.00
100	0.99	0.06	0.10	0.09	9.90
200	0.81	0.10	0.16	0.15	5.06
500	0.48	0.22	0.34	0.32	1.41
1000	0.28	0.24	0.38	0.35	0.74
2000	0.17	0.25	0.40	0.36	0.43
4000	0.14	0.25	0.41	0.36	0.34

TABLE 6. Fault line selection based on fixed frequency and amplitude comparison in neutral resonant grounding system.

R_G/Ω	I_1/A	I_2/A	I_3/A	I_4/A	K_S
50	1.03	0.03	0.06	0.05	17.17
100	0.88	0.13	0.20	0.19	4.40
200	0.70	0.18	0.29	0.26	2.41
500	0.23	0.30	0.47	0.43	0.49
1000	0.15	0.35	0.53	0.51	0.28
2000	0.13	0.36	0.55	0.52	0.24
4000	0.12	0.36	0.56	0.52	0.21

resistance of the neutral point ungrounded system reaches nearly 1000 Ω and the neutral point resonant grounding system reaches nearly 500 Ω , the method in [26]–[29] cannot achieve accurate line selection. When the grounding transition resistance is large and the frequency selection is not appropriate, the proportion of injected signal shunting into the normal line will increase. The anti-interference ability of this line selection is poor.

The simulation results of line selection using frequency dynamic selection and active power consumption are shown in Tab. 7 and Tab. 8. Where, the active power values of each line are P_1, P_2, P_3 and P_4 respectively. The corresponding K_f value satisfies equation (22), which means that fault line selection can be carried out accurately. Under the two operation modes of neutral point, the fault grounding resistance of 4000 Ω can be reached, and the fault line selection can still be accurate. Because of this method, the frequency of the injected signal is no longer a fixed value, and it has strong adaptability to different systems. In addition, the active power consumption of the injected signal in each line is used to select the fault line. The error caused by the normal line to the injected signal shunting is greatly suppressed. In the simulation, the K_f value is much larger than the set reference value. Even when the grounding resistance is large, the fault line selection can be realized.

TABLE 7. Fault line selection based on dynamic frequency and power comparison in ungrounded neutral system.

R_G/Ω	P_1/W	P_2/W	P_3/W	P_4/W	K_f
50	21.96	0.03	0.08	0.04	274.50
100	77.81	0.07	0.29	0.09	268.31
200	122.57	0.10	0.57	0.12	245.04
500	113.65	0.14	0.88	0.21	129.15
1000	73.49	0.41	1.60	0.49	45.93
2000	50.96	0.82	1.92	0.96	26.54
4000	27.86	1.93	2.15	2.07	12.96

TABLE 8. Fault line selection based on dynamic frequency and power comparison in neutral resonant grounding system.

R_G/Ω	P_1/W	P_2/W	P_3/W	P_4/W	K_f
50	18.61	0.03	0.12	0.04	155.08
100	41.09	0.17	0.59	0.19	69.64
200	68.56	0.30	1.31	0.37	52.34
500	87.64	0.51	1.64	0.64	53.44
1000	63.82	0.81	2.18	0.89	29.28
2000	40.19	1.32	2.62	1.56	15.34
4000	19.25	2.63	3.03	2.87	6.35

VIII. LABORATORY EXPERIMENT

A 600V four outlet analog distribution network system is built in the laboratory. The overall structure of the experimental system is shown in Fig. 1 and the experimental site is shown in Fig. 14. A high-power resistor is connected to one of the lines to simulate the single-phase ground fault. Then the whole system is short-term grounded. The power supply is disconnected immediately after the fault line selection is completed.

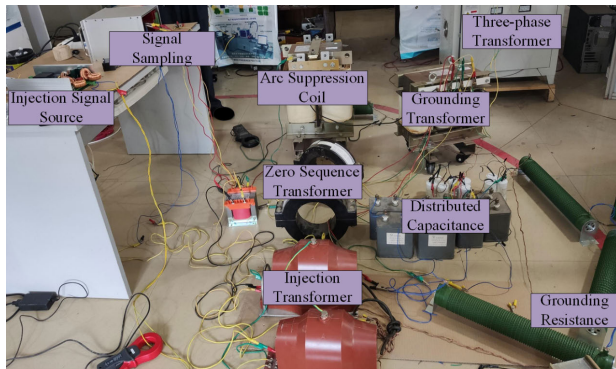


FIGURE 14. Experimental setup.

TABLE 9. Experimental results of fault line selection in 600 V resonant distribution network.

R_G/Ω	P_r/W	P_s/W	P_3/W	P_2/W	K_f
1000	68.71	1.13	1.59	1.26	43.21
2000	46.49	1.73	2.07	1.61	22.46
3000	21.23	1.94	2.23	1.89	9.52

In the experiments, the resonant grounding system with large distributed capacitance was tested. This is because tests with arc suppression coil are safer to conduct in laboratory due to its current suppression characteristics. More importantly, the line selection in arc suppression coil presents the most challenge to line selection. Therefore, it is more suitable to verify the effectiveness of the proposed method.

The analog distribution network system consists of a three-phase transformer, as shown in Fig. 14, which outputs three-phase 600V voltage. Then connects to the grounding transformer to lead out the neutral point of the distribution network. The arc suppression coil and injection transformer are connected at the neutral point, and the injection signal source is connected through the injection transformer. Zero-sequence transformer is added to each line for signal sampling. The injected signal is equivalent to zero-sequence signal in three phases of each line. Therefore, zero-sequence transformer can be directly used to extract the signal of injection frequency after taking zero-sequence signal of each line. Each line is connected with capacitors to emulate the distributed capacitance of distribution network, while different power resistors are used to emulate grounding transition resistance. When the grounding resistance of 3000 Ω is simulated, three high-power resistors with rated resistance of 1000 Ω are adopted in series.

The high-power resistor used in this experiment can overload 10 times for a short time and consume 5 seconds, which meets the requirements of this experiment. According to the simulation results in Fig. 11, the grounding current in the grounding resistance is 3 to 5 times of the rated value at the moment of the fault. But the duration is only a few hundred microseconds. After the arc suppression coil compensation process enters the steady state, the power resistance works within the rated power. Therefore, the experiment can be carried out.

The experimental results are shown in Tab. 9. The reliability of the fault line selection method is verified. The accurate line selection can still be realized in large capacity distribution network with 3000 Ω high resistance grounding.

IX. CONCLUSION

In this article, a new fault line selection scheme based on signal injection method for single-phase to ground fault line selection in small current grounding system is proposed and verified:

1) Signal injection method can solve the problems of low accuracy of steady-state method in line selection of resonant system and difficulty of transient fault instantaneous complete sampling. The injection time and sampling of injection method are controllable and not affected by fault degree and environment.

2) The dynamic selection of injection frequency has strong adaptability to the changes of distribution network system. The injection signal can flow into fault line as much as possible.

3) APFFT processes the sampled signal, highlights the main lobe, suppresses the side lobe, and reduces the error caused by spectrum leakage. Its horizontal phase characteristics ensure the accuracy of phase.

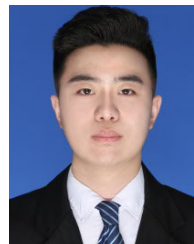
4) The criterion of line selection does not compare the amplitude of the injected signal, but the active power of the injected signal after the fault, which improves the accuracy of fault line selection.

5) The fault line selection method based on signal injection proposed in this article can realize the fault line selection under the condition of high resistance grounding interference. Future work is to use the injected signal to realize high-precision fault location, which makes the fault point removal even faster.

REFERENCES

- [1] Z. Yang and W. Wangdong, "Application of neutral point earthed method in medium voltage power grid," in *Proc. Int. Conf. Power Syst. Technol.*, Chongqing, China, Oct. 2006, pp. 1–5, doi: [10.1109/ICPST.2006.321737](https://doi.org/10.1109/ICPST.2006.321737).
- [2] H. Cao, G. Cai, H. Shi, and Y. Zhang, "Study on installing small reactance in neutral point of 500kV transformer on guangdong power grid," in *Proc. Int. Conf. Electr. Control Eng.*, Yichang, China, Sep. 2011, pp. 2594–2597, doi: [10.1109/ICECENG.2011.6058464](https://doi.org/10.1109/ICECENG.2011.6058464).
- [3] H. Zeng, P. Yang, H. Cheng, J. Xin, W. Lin, W. Hu, M. Wan, Y. Li, and H. Wu, "Research on single-phase to ground fault simulation base on a new type neutral point flexible grounding mode," *IEEE Access*, vol. 7, pp. 82563–82570, 2019, doi: [10.1109/ACCESS.2019.2922361](https://doi.org/10.1109/ACCESS.2019.2922361).
- [4] Y. Su, Y. Xue, B. Xu, and D. Liu, "The transient analysis of electronic arc-suppression coil and its effect on transient based fault line selection for single phase to Earth fault," in *Proc. Int. Conf. Adv. Power Syst. Autom. Protection*, Beijing, China, Oct. 2011, pp. 2410–2416, doi: [10.1109/APAP.2011.6180842](https://doi.org/10.1109/APAP.2011.6180842).
- [5] M. Pignati, L. Zanni, P. Romano, R. Cherkaoui, and M. Paolone, "Fault detection and faulted line identification in active distribution networks using synchrophasors-based real-time state estimation," *IEEE Trans. Power Del.*, vol. 32, no. 1, pp. 381–392, Feb. 2017, doi: [10.1109/TPWRD.2016.2545923](https://doi.org/10.1109/TPWRD.2016.2545923).
- [6] L. Shilong, T. Yufei, L. Xiaopeng, Z. Huajie, and F. Shilin, "Fault line selection of single phase grounding fault in small-current ground system based on reactive current," in *Proc. IEEE Innov. Smart Grid Technol. Asia (ISGT Asia)*, Chengdu, China, May 2019, pp. 138–143, doi: [10.1109/ISGT-Asia.2019.8881442](https://doi.org/10.1109/ISGT-Asia.2019.8881442).

- [7] M. Salehi and F. Namdari, "Fault classification and faulted phase selection for transmission line using morphological edge detection filter," *IET Gener., Transmiss. Distrib.*, vol. 12, no. 7, pp. 1595–1605, Apr. 2018, doi: [10.1049/iet-gtd.2017.0999](https://doi.org/10.1049/iet-gtd.2017.0999).
- [8] S. Huang, L. Luo, and K. Cao, "A novel method of ground fault phase selection in weak-infeed side," *IEEE Trans. Power Del.*, vol. 29, no. 5, pp. 2215–2222, Oct. 2014, doi: [10.1109/TPWRD.2014.2322073](https://doi.org/10.1109/TPWRD.2014.2322073).
- [9] C. H. Kim and R. K. Aggarwal, "Closure on 'a novel fault detection technique of high impedance arcing faults in transmission lines using the wavelet transform'," *IEEE Trans. Power Del.*, vol. 18, no. 4, pp. 1596–1597, Oct. 2003, doi: [10.1109/TPWRD.2003.817772](https://doi.org/10.1109/TPWRD.2003.817772).
- [10] C. Aguilera, E. Orduna, and G. Ratta, "Fault detection, classification and faulted phase selection approach based on high-frequency voltage signals applied to a series-compensated line," *IEE Proc. Gener., Transmiss. Distrib.*, vol. 153, no. 4, pp. 469–475, Jul. 2006, doi: [10.1049/ip-gtd:20045157](https://doi.org/10.1049/ip-gtd:20045157).
- [11] S. Luo, H. Gao, Y. Wu, J. Huang, and D. Wang, "Fast phase selection method based on transient current for UHV transmission lines," *J. Eng.*, vol. 2018, no. 15, pp. 938–943, Oct. 2018, doi: [10.1049/joe.2018.0269](https://doi.org/10.1049/joe.2018.0269).
- [12] P. Rajaraman, N. A. Sundaravaradan, R. Meyur, M. J. B. Reddy, and D. K. Mohanta, "Fault classification in transmission lines using wavelet multiresolution analysis," *IEEE Potentials*, vol. 35, no. 1, pp. 38–44, Jan. 2016, doi: [10.1109/MPOT.2015.2468775](https://doi.org/10.1109/MPOT.2015.2468775).
- [13] X. Song, F. Gao, Z. Chen, and W. Liu, "A negative selection algorithm-based identification framework for distribution network faults with high resistance," *IEEE Access*, vol. 7, pp. 109363–109374, 2019, doi: [10.1109/ACCESS.2019.2933566](https://doi.org/10.1109/ACCESS.2019.2933566).
- [14] Z. Dong, J. Peng, Z. Yang, and P. Huo, "Research and analysis of signal injection method for measuring capacitive current in distribution network," in *Proc. IEEE 3rd Int. Electr. Energy Conf. (CIEEC)*, Beijing, China, Sep. 2019, pp. 1495–1498, doi: [10.1109/CIEEC47146.2019.CIEEC-2019541](https://doi.org/10.1109/CIEEC47146.2019.CIEEC-2019541).
- [15] S. Zi-zheng and Q. Li-jun, "Study on automatic arc suppression coil compensation technology and fault line selection and location based on fixed-frequency signal injection method," in *Proc. 2nd Int. Conf. Artif. Intell., Manage. Sci. Electron. Commerce (AIMSEC)*, Dengleng, Aug. 2011, pp. 4354–4357, doi: [10.1109/AIMSEC.2011.6010035](https://doi.org/10.1109/AIMSEC.2011.6010035).
- [16] Z. Ming and H. Xu, "Fast line selection method of medium resistance in ARC suppression coil grounding system," *Power Syst. Technol.*, vol. 33, no. 12, pp. 112–114, Jun. 2009.
- [17] D. Zhou, "Research on grounding mode of 10 kV distribution network neutral point through arc suppression coil parallel resistance," *Shandong Ind. Technol.*, vol. 11, no. 11, pp. 206–208, Jun. 2016, doi: [10.16640/j.cnki.37-1222/t.2016.11.190](https://doi.org/10.16640/j.cnki.37-1222/t.2016.11.190).
- [18] Y. Sheng, M. Zhu, and X. Hu, "Discussion on operation safety and reliability of neutral point grounding through arc suppression coil and parallel line selection resistance in distribution network," *Energy Eng.*, vol. 5, no. 5, pp. 18–22, Oct. 2011, doi: [10.16189/j.cnki.nygc.2011.05.011](https://doi.org/10.16189/j.cnki.nygc.2011.05.011).
- [19] Z. Gao, H. Zhang, and X. Sun, "Fault line selection and location method for small current grounding with half wave DC injection," *Power Syst. Protection Control*, vol. 41, no. 13, pp. 139–145, Jun. 2013.
- [20] J. Zhou, N. Liu, and S. Li, "Fault line selection for small current grounding based on equivalent half wave injection method," *Electr. Meas. Instrum.*, vol. 57, no. 4, pp. 55–60, Jul. 2020, doi: [10.19753/j.issn1001-1390.2020.04.009](https://doi.org/10.19753/j.issn1001-1390.2020.04.009).
- [21] G. Yan, G. Li, Z. Zhang, L. Xiao, J. Cao, G. Mu, and W. Dai, "Development of capacitive current measurement device for distribution network based on sweep frequency method," *Electr. Power Automat. Equip.*, vol. 3, no. 3, pp. 64–68, Apr. 2007.
- [22] L. Lin and Y. Liu, "A capacitive current detection system to ground based on frequency conversion signal method," *Power Syst. Protection Control*, vol. 23, no. 42, pp. 44–49, Nov. 2014.
- [23] L. Jiansheng and L. Jun, "10kV straight line fault location based on 'signal injection method,'" in *Proc. IEEE Power Eng. Autom. Conf.*, Sep. 2011, pp. 512–515, doi: [10.1109/PEAM.2011.6134987](https://doi.org/10.1109/PEAM.2011.6134987).
- [24] Z. Liang, Y. Wang, and B. Wang, "Research on fault location of single phase to ground fault in distribution line based on injected signal," *Digit. Technol. Appl.*, vol. 12, no. 12, pp. 79–80, Dec. 2015, doi: [10.19695/j.cnki.cn12-1369.2015.12.062](https://doi.org/10.19695/j.cnki.cn12-1369.2015.12.062).
- [25] F. Wang, Z. Fu, and J. Duan, "Research on on line detection instrument of mine low voltage cable insulation parameters," *Proc. CSU-EPSCA*, vol. 4, no. 4, pp. 48–51, Aug. 2000.
- [26] H. Zhang, Z. Pan, and Z. Tian, "Ground fault detection method of distribution network based on injection method," *J. Univ. Jinan*, vol. 2, no. 2, pp. 164–168, May 2004, doi: [10.13349/j.cnki.jdxbn.2004.02.022](https://doi.org/10.13349/j.cnki.jdxbn.2004.02.022).
- [27] Z. Sang, Z. Pan, and L. Li, "A new technology of single phase grounding fault location and location in small current grounding system," *Power Syst. Technol.*, vol. 10, no. 10, pp. 50–52, Oct. 1997, doi: [10.13335/j.1000-3673.pst.1997.10.016](https://doi.org/10.13335/j.1000-3673.pst.1997.10.016).
- [28] J. Wang and Z. Zhang, "Research on fault line selection of small current grounding based on injected signal and wavelet energy," *Power Syst. Technol.*, vol. 55, no. 05, pp. 28–32, Mar. 2018.
- [29] Y. Cheng, L. Song, and W. Wang, "Research and implementation of 35kV line fault location system," *Power Syst. Protection Control*, vol. 8, no. 8, pp. 16–20, Apr. 2007.
- [30] S. Wang, R. Inkol, S. Rajan, and F. Patenaude, "Detection of narrow-band signals through the FFT and polyphase FFT filter banks: Noncoherent versus coherent integration," *IEEE Trans. Instrum. Meas.*, vol. 59, no. 5, pp. 1424–1438, May 2010, doi: [10.1109/TIM.2009.2038294](https://doi.org/10.1109/TIM.2009.2038294).
- [31] S. Liu, N. Lyu, J. Cui, and Y. Zou, "Improved blind timing skew estimation based on spectrum sparsity and ApFFT in time-interleaved ADCs," *IEEE Trans. Instrum. Meas.*, vol. 68, no. 1, pp. 73–86, Jan. 2019, doi: [10.1109/TIM.2018.2834080](https://doi.org/10.1109/TIM.2018.2834080).
- [32] J. Tian, J. Sun, G. Wang, Y. Wang, and W. Tan, "Multiband radar signal coherent fusion processing with IAA and apFFT," *IEEE Signal Process. Lett.*, vol. 20, no. 5, pp. 463–466, May 2013, doi: [10.1109/LSP.2013.2251631](https://doi.org/10.1109/LSP.2013.2251631).
- [33] J. Zhao, Y. Zhou, J. Zhao, J. Song, and F. Dong, "Precision position measurement of PMSLM based on ApFFT and temporal sinusoidal fringe pattern phase retrieval," *IEEE Trans. Ind. Informat.*, vol. 16, no. 12, pp. 7591–7601, Dec. 2020, doi: [10.1109/TII.2020.2967543](https://doi.org/10.1109/TII.2020.2967543).
- [34] Y. Pan, T. Zhang, G. Zhang, and Z. Luo, "A novel acquisition algorithm based on PMF-apFFT for BOC modulated signals," *IEEE Access*, vol. 7, pp. 46686–46694, 2019, doi: [10.1109/ACCESS.2019.2909787](https://doi.org/10.1109/ACCESS.2019.2909787).



LIN NIU was born in Henan, China, in 1997. He received the B.S. degree in electrical engineering from the Henan University of Technology, Zhengzhou, China, in 2019. He is currently pursuing the M.S. degree with the College of Electrical and Information Engineering, Hunan University. His research interests include power electronics and safe operation and control of distribution networks.



GUIQING WU was born in Hunan, China, in 1966. He received the B.S. degree in radio technology from Northwest Polytechnic University, in 1988, and the M.S. degree in measurement and control instrument and the Ph.D. degree in circuit and system from Hunan University, Changsha, China, in 1994 and 2012, respectively.

In 1994, he joined the College of Electrical and Information Engineering, Hunan University, where he is currently a Professor. He has published more than 80 articles in journals, and obtained 13 invention patents and utility model patents. His research interests include power electronics and switching power supply.



ZHANGSHENG XU was born in Hunan, China, in 1996. He received the B.S. degree in electronic science and technology from the Hunan University of Arts and Science, Changde, China, in 2018. He is currently pursuing the M.S. degree with the College of Electrical and Information Engineering, Hunan University. His research interest includes distribution network fault detection.

• • •